Time Domain Modeling of Impedance Boundary Condition

C. F. Lee, R. T. Shin, and J. A. Kong

Abstract—**A methodology developed to handle dispersive materials in the time domain is extended to model the dispersive characteristics of the impedance boundary condition used for a thin layer coating over perfect conductors. The impedance boundary condition is first approximated as a rational function of frequency. This rational function is then transformed to a time domain equation, resulting in a partial differential equation in space and time. Discretization of the time domain model to efficiently handle the thin layer coating is presented in the context of the finite-difference time-domain (FD-TD) technique. The methodology is verified by solving a one-dimensional problem using the FD-TD technique and comparing with the analytical results.**

I. Introduction

Electrically fine structures often appear in practical applications. To resolve the electromagnetic behavior of these structures, very fine grids are needed in numerical techniques (e.g., the finite-difference time-domain technique). Alternatively, one may incorporate the localized physical behavior, such as the impedance boundary condition [1] and thin wire formulations [2], [3], of these fine structures into discretization schemes.

Thin surface coatings on metallic bodies appear in many scattering problems. In principle, these thin surface coatings can be modeled numerically and geometrically by very fine grids with appropriate discretization schemes. The disadvantage associated with such an approach is the large computer memory requirement. Furthermore, in the finite-difference time-domain (FD-TD) technique, the time increment is usually determined by the smallest grid size in the entire computational domain to satisfy the stability condition.

In modeling a thin layer coating in the frequency domain, the concept of impedance boundary condition can be used to avoid the fine layers of grids. The impedance boundary condition relates the tangential fields on the coating to their normal derivatives, which is derived using the configuration of a half-space conductor with thin layer coating. The resulting impedance boundary condition is frequency dependent, and this dispersive nature of the impedance boundary condition causes difficulty in the time domain modeling. In this paper, a time domain technique used to treat dispersive materials is employed to convert the impedance boundary condition to the time domain [4]. Following the idea in [5], the impedance boundary condition is approximated by a rational function of the frequency. Then, the tangential fields are related to their normal derivatives by a partial differential equation in space and time. A numerical discretization scheme in the context of the FD-TD technique is discussed and the overall scheme is verified numerically for a one-dimensional configuration.

Manuscript received September 9, 1991; revised February 10, 1992. This work was supported in part by ONR Contract N00014-90-J-1002 and the Joint Services Electronics Program under the Contract DAAL03-89-C-0001.

C. F. Lee is with WaveTracer, Inc., Acton, MA 01720.

R. T. Shin and J. A. Kong are with the Department of Electrical and Engineering and Computer Science, and Research Laboratory of Electronics, Massachusetts Institute of Technology, Cambridge, MA 02139.

IEEE Log Number 9201728.

II. Time Domain Description of the Impedance Boundary Condition

The impedance boundary condition of the coated conductor can be derived based on a two-layer configuration (Fig. 1). By ignoring the variation along the tangential directions, the tangential electric field can be related to its normal derivative by the following equation:

$$E = \frac{\eta_r}{k} \tan\left(k\,\Delta\sqrt{\mu_r\epsilon_r}\right)\frac{\partial E}{\partial y}, \tag{1}$$

where k is the free space wavenumber, μ_r and ϵ_r are the relative permeability and relative permittivity, respectively, and $\eta_r = \sqrt{\mu_r/\epsilon_r}$ is the relative impedance (impedance normalized to η_0). Inverse Fourier transformation may be used to convert the above equation to the time domain. However, it is relatively complicated and the result may not be suitable for numerical analysis. Instead, following the procedure outlined in [5], the above equation is approximated using a rational function of the frequency. With the substitution of $-i\omega$ by $\partial/\partial t$, the time domain description of the impedance boundary condition is obtained.

The rational function approximated of (1) can be obtained by expressing the *tangent* function as the ratio of *sine* and *cosine*. Next, the Taylor series expansions of these two functions are used to obtain the rational function form. By keeping the first two terms in the Taylor series expansions of the *sine* and *cosine* functions, the first-order rational function approximation is obtained,

$$E = \eta_r\,\Delta\sqrt{\mu_r\epsilon_r}\,\frac{1-\frac{1}{6}k^2\,\Delta^2\mu_r\epsilon_r}{1-\frac{1}{2}k^2\,\Delta^2\mu_r\epsilon_r}\frac{\partial E}{\partial y}. \tag{2}$$

Similarly, by keeping the first three terms of Taylor series expansion, the second-order approximation can be obtained:

$$E = \eta_r\,\Delta\sqrt{\mu_r\epsilon_r}\,\frac{1-\frac{1}{6}k^2\,\Delta^2\mu_r\epsilon_r+\frac{1}{120}k^4\,\Delta^4\mu_r^2\epsilon_r^2}{1-\frac{1}{2}k^2\,\Delta^2\mu_r\epsilon_r+\frac{1}{24}k^4\,\Delta^4\mu_r^2\epsilon_r^2}\frac{\partial E}{\partial y}. \tag{3}$$

In general, both the relative permittivity and permeability in (2) and (3) can be complex to account for electric and magnetic losses. However, in this paper, we will consider only the loss due to electrical conductivity.

The time domain expressions corresponding to (2) and (3) can be obtained by substituting $-i\omega$ by $\partial/\partial t$, or equivalently, $-ik$ by $\partial/\partial\tau$, where $\tau = c_0 t$ is the normalized time. Assuming electrical conduction loss only, we obtain

$$\epsilon_r = \epsilon' + i\frac{\sigma\eta_0}{k}, \tag{4}$$

where ϵ', σ and η_0 are dielectric constant, electric conductivity and free space impedance, respectively. The first-order time domain description of the impedance boundary condition corresponding to

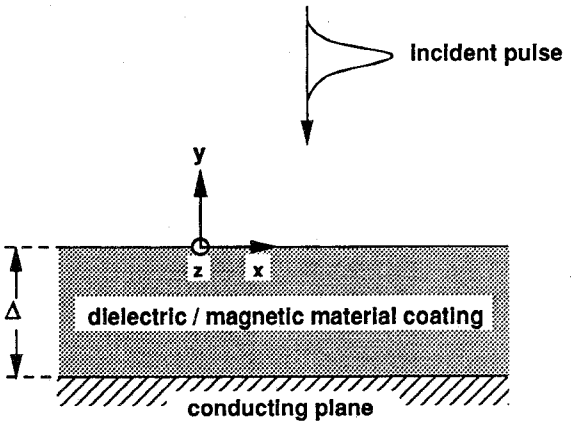

Fig. 1. Two-layer configuration.

(2) is given by

$$\left[1 + \frac{1}{2}\mu_r \Delta^2 \sigma \eta_0 \frac{\partial}{\partial \tau} + \frac{1}{2}\Delta^2 \epsilon' \mu_r \frac{\partial^2}{\partial \tau^2}\right] E = \Delta \left[1 + \frac{1}{6}\mu_r \Delta^2 \sigma \eta_0 \frac{\partial}{\partial \tau} + \frac{1}{6}\Delta^2 \epsilon' \mu_r \frac{\partial^2}{\partial \tau^2}\right] \frac{\partial E}{\partial y} \quad (5)$$

Applying the same transformation to (3), the second-order time domain description of the impedance boundary condition is given by

$$\left[1 + \frac{1}{2}\Delta^2 \sigma \eta_0 \frac{\partial}{\partial \tau} + \left(\frac{1}{2}\Delta^2 \epsilon' + \frac{1}{24}\Delta^4 \sigma^2 \eta_0^2\right)\frac{\partial^2}{\partial \tau^2} + \frac{1}{12}\delta^4 \epsilon' \sigma \eta_0 \frac{\partial^3}{\partial \tau^3} + \frac{1}{24}\Delta^2 \epsilon'^2 \frac{\partial^4}{\partial \tau^4}\right] E = \Delta \left[1 + \frac{1}{6}\Delta^2 \sigma \eta_0 \frac{\partial}{\partial \tau} + \left(\frac{1}{6}\Delta^2 \epsilon' + \frac{1}{120}\Delta^4 \sigma^2 \eta_0^2\right)\frac{\partial^2}{\partial \tau^2} + \frac{1}{60}\Delta^4 \epsilon' \sigma \eta_0 \frac{\partial^3}{\partial \tau^3} + \frac{1}{120}\Delta^4 \epsilon'^2 \frac{\partial^4}{\partial \tau^4}\right] \frac{\partial E}{\partial y} \quad (6)$$

The above time domain descriptions of the impedance boundary condition are partial differential equations in space and time. In fact, these equations may be derived directly in the time domain with a finite difference approximation and a simple averaging scheme [4] (see Appendix). The impedance boundary condition accounts for the interaction between air-dielectric interface and conducting surface. In the time domain there is a time delay associated with this interaction. This delay is partially modeled by (5) and (6).

III. Discretization

There are many discretization schemes one can use to discretize (5) and (6) for the finite-difference time-domain technique. The discretization of the normal derivative is quite important in the implementation of the impedance boundary condition. In order to have an accurate approximation, the vanishing tangential electric field on the conducting surface is used. This leads to interpolation of the electric field in three or more locations. Employing the Lagrange interpolation formula for three electric fields (Fig. 2), the normal derivative is discretized as follows:

$$\left.\frac{\partial E}{\partial y}\right|_1 = \frac{a}{\Delta_y (1 + a)}\left[E_2 \frac{a^2 - 1}{a^2} E_1\right]. \quad (7)$$

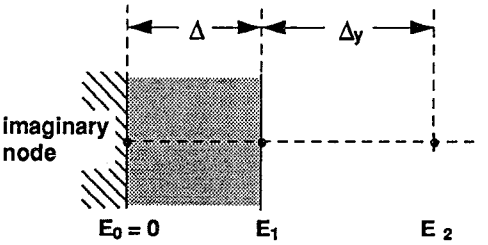

Fig. 2. Discretization nodes for normal derivative.

In the above equation a represents the ratio of the layer thickness to the grid size, Δ/Δ_y. It turns out that a better approximation of the normal derivative can be obtained by including the effect of the dielectric constant of the coating. Because the wave velocity in the coating is slower than that in the free space where discretization applied, the effective thickness of the coating should be $\Delta\sqrt{\epsilon'}$. Therefore, the following equation is used:

$$a = \frac{\Delta\sqrt{\epsilon'}}{\Delta_y}.$$

The temporal derivatives in (5) and (6) may also be discretized in many forms. A simple second-order center-differencing is used in this paper.

IV. Numerical Results

Equations (5) and (6) describe the time domain modeling of the impedance boundary condition given by (1). Equation (7) and center-differencing in time provide a possible discretization scheme. To validate the approach outlined in this paper, a one-dimensional reflection problem is simulated using these models together with the finite-difference time-domain method [3]. The reflected wave is calculated in the time domain and Fourier transformed to obtain the reflection coefficient as a function of frequency. The results are compared with the exact solution obtained directly in the frequency domain.

Fig. 1 shows the configuration of the problem. The layer has thickness of 0.2 cm. The coating material is assumed to have dielectric constant of 5 and conductivity of 0.2 mho/meter. The computation domain contains 500 nodes with grid size being 0.2 cm. The normalized time increment Δ_τ is 0.2 cm to satisfy the stability criterion and to minimize numerical dispersion. At the first node of the computational domain, an incident Gaussian pulse modulated by a carrier at 8 GHz is imposed. This Gaussian pulse has a half-power pulse width of 0.0625 nano-second, which corresponds to a bandwidth of 6 GHz. The last node of the computational domain is placed at the free space/dielectric interface where the first-order or the second-order approximation to the impedance boundary condition (IBC) is applied to simulate the thin layer coating.

The exact solution for the reflection coefficient is given by

$$R(k) = \frac{i\eta_r \tan(k\,\Delta\sqrt{\mu_r \epsilon_r}) + 1}{i\eta_r \tan(k\,\Delta\sqrt{\mu_r \epsilon_r}) - 1}, \quad (8)$$

where η_r and ϵ_r is complex. For the assumed parameters, the magnitude and the phase of this reflection coefficient are plotted in Fig. 3(a) and (b) (solid curves), respectively, from 2 GHz to 16 GHz. The results obtained by using the FD-TD simulation are also shown in Fig. 3(a) and (b). The "○" and "+" curves represent results

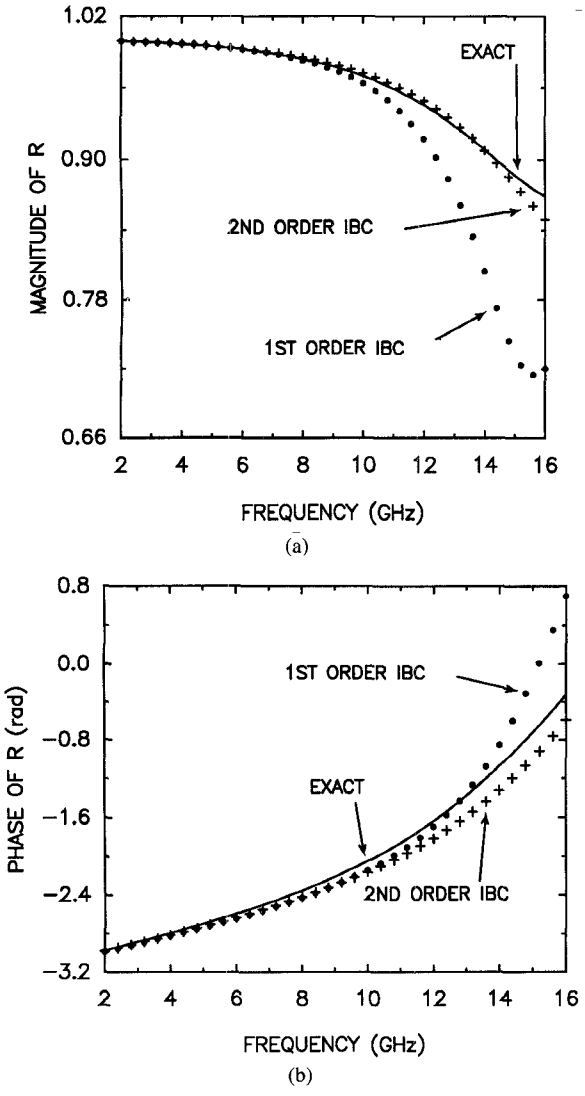

Fig. 3. (a) Magnitude of reflection coefficient versus frequency. (b) Phase of reflection coefficient versus frequency.

obtained using (5) and (6), respectively. Both the first- and the second-order approximations yield good agreement with the exact solution in the phase of the reflection coefficient. However, the advantage of using the second-order approximation, (6), is clearly shown in the magnitude of the reflection coefficient. The results obtained using the first-order approximation match the exact solution at low frequencies with increasing discrepancy at higher frequencies.

Fig. 4 shows the percent error of the reflection coefficient magnitude as a function of the coating thickness. These errors are for the FD-TD results with the second-order approximation of the IBC using the same grid size and the same material parameters while varying the coating thickness. The three curves represent errors at three different frequencies. The errors for the half-power frequencies, 5 GHz and 11 GHz, are shown by "+" and "×," respectively. The errors at the carrier frequency are shown by "○." These errors are all well within 1.0 percent, and they increase with increasing thickness, as expected. It should be noted that the errors are relatively small even when the thickness of the coating is up to 1/5 of the wavelength inside the layer as in the case of 11 GHz at the thickness of 0.25 cm.

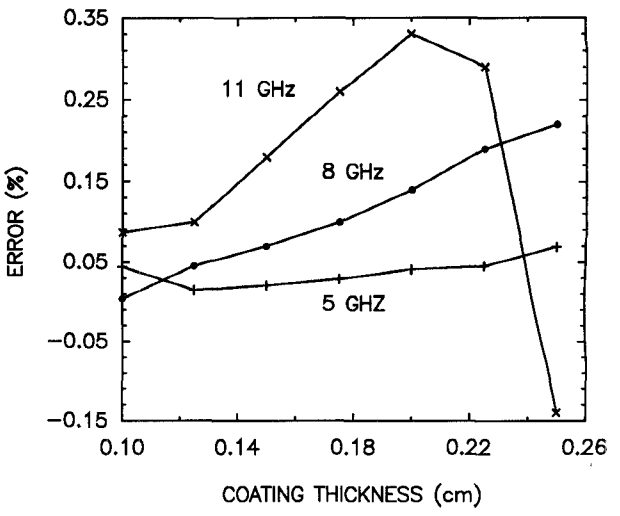

Fig. 4. Percentage error for second-order IBC versus coating thickness.

V. Summary

In this paper, a time domain modeling of the impedance boundary condition is derived and expressed in terms of partial differential equations in space and time. A possible discretization scheme which incorporates the effective thickness of the layer is presented. Numerical results indicate the validity of the modeling as well as the suggested discretization scheme. Although this model is only verified for a one-dimensional problem, the generalization to higher spatial dimensions is possible since the equation is applied only at the interface. However, tangential variations may need to be considered in those cases. Furthermore, the concept of using the rational functions to approximate the frequency domain response and converting to the time domain may be used to characterize other fine structures.

Appendix

For simplicity, the relative permittivity and permeability are assumed real. For a plane wave normally incident with waveform g,

$$E_i = g(\tau + y), \quad \eta_0 H_i = -g(\tau + y). \tag{A1}$$

the reflected and transmitted waves are

$$E_r = f(\tau - y), \quad \eta_0 H_r = f(\tau - y); \tag{A2}$$

$$E_s = p(\tau + \sqrt{\mu_r \epsilon_r}\, y + \sqrt{\mu_r \epsilon_r}\, \Delta) - p(\tau - \sqrt{\mu_r \epsilon_r}\, y - \sqrt{\mu_r \epsilon_r}\, \Delta); \tag{A3a}$$

$$\eta_0 H_s = -\frac{1}{\eta_r} p(\tau + \sqrt{\mu_r \epsilon_r}\, y + \sqrt{\mu_r \epsilon_r}\, \Delta) - \frac{1}{\eta_r} p(\tau - \sqrt{\mu_r \epsilon_r}\, y - \sqrt{\mu_r \epsilon_r}\, \Delta); \tag{A3b}$$

In (A2) and (A3), the subscripts r and s denote the reflected wave and the wave inside the coating, respectively. Note that the boundary condition on the surface of the conductor has been satisfied. Imposing the boundary conditions of continuous tangential electric and magnetic fields at the interface,

$$E = g(\tau) + f(\tau) = p(\tau + \sqrt{\mu_r \epsilon_r}\, \Delta) - p(\tau - \sqrt{\mu_r \epsilon_r}\, \Delta), \tag{A4a}$$

$$\eta_0 H = g(\tau) + f(\tau) = -\frac{1}{\eta_r} p(\tau + \sqrt{\mu_r \epsilon_r}\,\Delta)$$

$$-\frac{1}{\eta_r} p(\tau - \sqrt{\mu_r \epsilon_r}\,\Delta). \quad \text{(A4b)}$$

In addition, the total tangential electric and magnetic fields are related by:

$$E = 2g(\tau) + \eta_0 H. \quad \text{(A5)}$$

Applying the center-differencing and averaging approximations:

$$p(\tau + \sqrt{\mu_r \epsilon_r}\,\Delta) - p(\tau - \sqrt{\mu_r \epsilon_r}\,\Delta)$$
$$\sim 2\Delta\sqrt{\mu_r \epsilon_r}\, p'(\tau) + \tfrac{1}{3}\Delta^3 (\mu_r \epsilon_r)^{3/2} p'''(\tau) \quad \text{(A6a)}$$

$$p(\tau + \sqrt{\mu_r \epsilon_r}\,\Delta) + p(\tau - \sqrt{\mu_r \epsilon_r}\,\Delta)$$
$$\sim 2p(\tau) + \Delta^2 \mu_r \epsilon_r p''(\tau), \quad \text{(A6b)}$$

where "'" denotes derivative with respect to the argument. Substituting these back into (A4),

$$2g(\tau) = \frac{2}{\eta_r} p(\tau) + 2\Delta\sqrt{\mu_r \epsilon_r}\, p'(\tau)$$
$$+ \frac{\Delta^2}{\eta_r} \mu_r \epsilon_r p''(\tau) + \frac{\Delta^3}{3} (\mu_r \epsilon_r)^{3/2} p'''(\tau) \quad \text{(A7)}$$

$$\eta_0 H = -\frac{1}{\eta_r} [2p(\tau) + \Delta^2 \mu_r \epsilon_r p''(\tau)]. \quad \text{(A8)}$$

Substituting (A7) and (A8) to (A5), E is related to the first and third derivatives of $p(\tau)$. Again, using (A8) and ignoring the terms involving derivatives higher than third order by assuming slowly varying field in the time scale of Δ_τ:

$$E = -\Delta \mu_r \frac{\partial \eta_0 H}{\partial \tau} + \frac{\Delta^3 \mu_r^2 \epsilon_r}{3} \frac{\partial^3 \eta_0 H}{\partial \tau^3}. \quad \text{(A9)}$$

Using Maxwell's equations:

$$E = \Delta \mu_r \frac{\partial E}{\partial y} - \frac{\Delta^3 \mu_r^2 \epsilon_r}{3} \frac{\partial^3 E}{\partial \tau^2\, \partial y}.$$

This is what one expects if one expands, in Taylor series, the *tangent* function in (1) and converts the expanded equation to the time domain using the procedure described earlier.

References

[1] T. B. A. Senior and J. L. Volakis, "Derivation and application of a class of generalized boundary conditions," *IEEE Trans. Antennas Propagat.*, vol. 37, pp. 1566–1572, Dec. 1989.

[2] R. Holland and L. Simpson, "Implementation and optimization of the thin-strut formulism in THREDE," *IEEE Trans. Nuclear Sci.*, vol. NS-6, pp. 1625–1630, 1980.

[3] A. Taflove, K. R. Umashankar, B. Beker, F. Harfoush, and K. S. Yee, "Detailed FD-TD analysis of electromagnetic fields penetrating narrow slots and lapped joints in thick conducting screens," *IEEE Trans. Antennas Propagat.*, vol. 36, p. 247–257, Feb. 1988.

[4] C. F. Lee, R. T. Shin, and J. A Kong, "Application of finite-difference time-domain techniques to dispersive media," *Progress in Electromagnetics Research Symp.* Cambridge, MA, July 1991.

[5] ——, *Progress in Electroamgnetic Research*, J. A. Kong, Ed., vol. 4, pp. 373–442, New York: Elsevier, 1991.

Comments on "Criteria for the Onset of Oscillation In Microwave Circuits"

Robert W. Jackson

The paper listed above[1] notes that the device reflection coefficient, $\Gamma_d(s)$, in the expression,

$$V^+ = \frac{\Gamma_d(s)}{1 - \Gamma_d(s)\Gamma_c(s)} V_i$$

represents the port reflection coefficient of a device which may result in an unstable circuit only *after* connecting it with a resonator having a reflection coefficient, $\Gamma_c(s)$. This is an important condition and is somewhat vague as worded. In order to use the Nyquist criterion to determine the stability of the device-circuit combination, Γ_d must have no right half plane poles. This amounts to insuring that the device does not oscillate into the reference impedance (50 ohms for example). If Γ_d has been determined from measurements, presumably the device is not oscillating during the measurement and therefore there are no right half plane poles.

In CAD simulations of possibly unstable circuits, the location of Γ_d poles is not always so clear. For a simple amplifier circuit such as the one described in the above referenced paper, one can assume no right half plane poles in Γ_d if the S_{11} and/or S_{22} coefficients of the FET have magnitudes less than one. To see this, consider the partial circuit formed by a 50 ohm termination on port 2 and any passive termination on port 1. If $|S_{11}| < 1$, the input termination sees a passive impedance and therefore the partial circuit is stable. Since the partial circuit is stable, Γ_d (50 ohm reference) seen looking in at port 2 has no poles in the right half plane. If, as in the amplifier example[1], Γ_d has a magnitude greater than 1, the Nyquist criterion as described can then be applied to study the stability effects of various port 2 terminations. In simulations using devices with extra feedback, oscillators for example, often the magnitudes of S_{11} and S_{22} are both greater than one and this approach breaks down.

A more generally applicable use of the Nyquist stability criterion has been known for years, but the current widespread use of microwave CAD makes it must easier to apply. As discussed in the literature [1], [2] the admittance between any two nodes in an active circuit cannot have right half plane zeros if the circuit is to be stable. If one were to apply the Nyquist test to such an admittance, the resulting Nyquist locus of points cannot encircle zero in a clockwise sense if the circuit is stable. It is trivial for modern microwave CAD programs to calculate the necessary admittances vs frequency. Polar plotting of admittances is not always available but a quick sketch is easy to do. It should be noted that the number of Nyquist encirclements only gives the *difference* between the number of right half plane zeros and poles in the admittance function. If, for example, the admittance at a particular node pair has an equal number of right half plane poles and zeros, the Nyquist plot would not encircle the origin even though the circuit is unstable. Thus a clockwise encirclement insures instability, but no encirclement does not insure stability. Since admittances at various node

[1] R. W Jackson, *IEEE Trans. Microwave Theory Tech.*, vol. 40, no. 3, pp. 566–568, Mar. 1992.